JOURNAL OF OPTIMIZATION THEORY AND APPLICATIONS: Vol. 9, No. 5, 1972

The Game of Two Identical Cars[1]

A. W. MERZ[2]

Communicated by Y. C. Ho

Abstract. This paper describes a third-order pursuit–evasion game in which both players have the same speed and minimum turn radius. The game of kind is first solved for the *barrier* or envelope of capturable states. When capture is possible, the game of degree is then solved for the optimal controls of the two players as functions of the relative position. The solution is found to include a universal surface for the pursuer and a dispersal surface for the evader.

1. Introduction

The two-car differential game problem was originally defined and examined by Isaacs in Ref. 1. In this pursuit–evasion game, the pursuer P and the evader E both have positive minimum-turn radii and constant speeds, and motion is restricted to a plane. The state vector of the game has three components, which are chosen as the Cartesian coordinates x, y of E's position relative to P and the angle θ between the two velocities. The game terminates when E's separation from P becomes less than a specified capture radius, and it is the termination time that P seeks to minimize and E to maximize. The general two-car problem has three independent parameters: the speed ratio and the two ratios of capture radius to minimum-turn radius.

The present study is a specialization to the case of two identical cars; i.e., both P and E have unit velocity and unit maximum turn rate, so that only one parameter remains, which is the ratio β of capture

[1] Paper received June 7, 1971; in revised form, September 15, 1971. The author is grateful to Professor J. V. Breakwell, Stanford University, for constructive criticism of the manuscript. Financial support for the research was provided at Stanford University under Air Force Contract No. F33615-70-C-1637.

[2] Postdoctoral Fellow, Department of Aeronautics and Astronautics, Stanford University. Presently, Research Engineer, Systems Control, Palo Alto, California.

radius to the common minimum-turn radius. It is assumed that the roles of P and E do not change during the game, so that, when capture can occur, a necessary condition to be satisfied by the saddle-point controls of the players is the Hamiltonian (which can be derived as in Ref. 1)

$$\min_{\sigma_1} \max_{\sigma_2} [V_x \dot{x} + V_y \dot{y} + V_\theta \dot{\theta} + 1] = 0. \tag{1}$$

Here, the controls are the normalized turn rates of P and E, σ_1 and σ_2, where $|\sigma_i| \leqslant 1$, which are to be found as functions of the state vector, $[x, y, \theta]$. The adjoint vector $[V_x, V_y, V_\theta]$ is known in terms of the terminal conditions of the game, so the overall game can be viewed generically as a two-point boundary-value problem.

1.1. Preliminary Remarks. Isaacs' treatment of this problem is restricted to the case of a faster pursuer, and is further limited to a study of the optimal strategies and trajectories on the *barrier*. This is a surface in $xy\theta$-space representing solutions to the *game of kind*. Across the barrier, the optimal time-to-go is discontinuous, and on this surface the optimal paths contact the capture circle tangentially, without penetrating, as shown in Fig. 9.2.3 of Ref. 1. For arbitrary parameter values, the barrier may be open or closed; and, when it is closed, capture or termination of the game is possible under optimal play only for those initial states bounded between the capture circle and the barrier.

In the specialized case analyzed here, capture does not necessarily occur, because the players' speeds and maximum turn rates are equal. If the initial velocities are parallel (for example, $\theta = 0$), the equations of relative motion show that E can maintain the initial radial separation forever, by simply duplicating P's strategy. The barrier is therefore closed, and the *game of kind* is concerned with the determination of this surface.

The calculation of the barrier begins with the determination of a terminal relation among the state components, which expresses the tangential relative velocity condition. Values of the normalized adjoints are also known in terms of the state at this time. The controls of both players at termination are thus known. Retrogressive integration of the state equations is then possible in terms of the terminal states. Sketching a typical pair of trajectories in realistic space, however, shows that, when E is sufficiently far from P on this path, E could avoid P entirely by adopting a different policy, despite the fact that neither player's switch function has changed sign at this retrograde time. This initially puzzling feature of the solutions was found to have a precedent in the second-order homicidal chauffeur game. In this game, for certain para-

meter values, the right and left barriers intersect ahead of the capture circle at an evader's dispersal point, and the barrier loci beyond this point are discarded (Ref. 1, p. 235). In the present third-order problem, the two barrier surfaces are found to intersect along an evader's dispersal *line*, and the retrograde solutions beyond this line are no longer optimal. The determination of this line is simple, in principle, though it requires consideration of rather complex simultaneous equations in practice. In the analysis to follow, important relations will often be given in functional form only, to avoid the explicit algebraic details involved in the barrier calculation.

When capture is possible, termination must occur with E entering the capture circle between the two barrier surfaces. Solutions to the *game of degree* are then found by first determining strategies for P and E as functions of the state at the time of capture. This results in four possible sets of terminal controls, each of which is optimal in a specific area of the terminal region of the state space. As with the game of kind, the corresponding sets of terminal conditions can be integrated retrogressively, away from the capture circle, so as to fill the capture volume with optimal trajectories. This procedure is complicated by the presence of a dispersal surface for E and a universal surface for P, but these surfaces intersect the capture circle along the lines which subdivide the terminal area, as mentioned above. Consequently, their influence on the shapes of the various strategy regions can be predicted qualitatively as these surfaces are generated away from the capture region. The actual calculation of these surfaces is by simultaneous numerical solution of a set of transcendental equations, which are the general solutions, in retrogressive time, to the differential equations of the game.

These surfaces essentially provide the solution to the game, by giving those states from which capture is possible, and by specifying optimal strategies for both players as functions of the state when capture is possible. The results are finally shown as $\theta = \text{const}$ sections of the three-dimensional state space, because this seems to be the simplest and clearest way of presenting these *strategy volumes*.

1.2. Equations of Motion and Terminal Conditions. With the notations shown in Fig. 1, the equations of relative motion of the game are found to be

$$\dot{x} = -\sigma_1 y + \sin\theta, \qquad \dot{y} = -1 + \sigma_1 x + \cos\theta, \qquad \dot{\theta} = -\sigma_1 + \sigma_2 . \quad (2)$$

Terminal conditions of the states are expressible as the vector

$$\mathbf{x}_0 = [\beta \sin\phi_0 , \beta \cos\phi_0 , \theta_0], \quad (3)$$

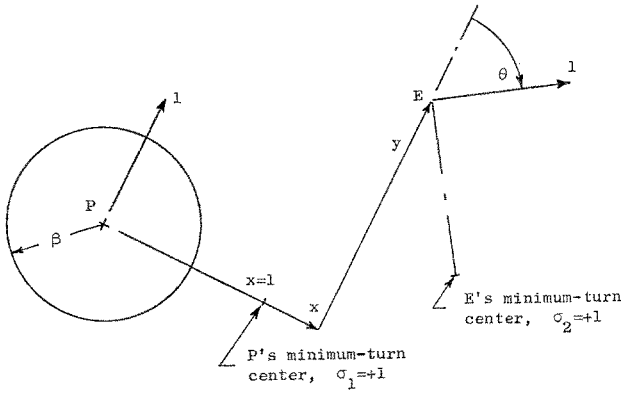

Fig. 1. Notations and coordinates.

where the polar coordinate ϕ_0 must be such that the radial velocity at termination is nonpositive. That is,

$$\dot{r}_0 = \cos(\theta_0 - \phi_0) - \cos\phi_0 \leqslant 0. \tag{4}$$

The terminal condition of the game of kind is given by the equality in (4), so that a *safe-contact* trajectory which touches the capture circle tangentially must satisfy either

$$\theta_0 = 2\phi_0 \tag{5}$$

or

$$\theta_0 = 0. \tag{6}$$

These terminal conditions denote the *boundary of the usable part* (or BUP), as shown in Fig. 2, and the game of degree terminates on the portion of the capture circle between these lines, where $\dot{r}_0 < 0$. Note

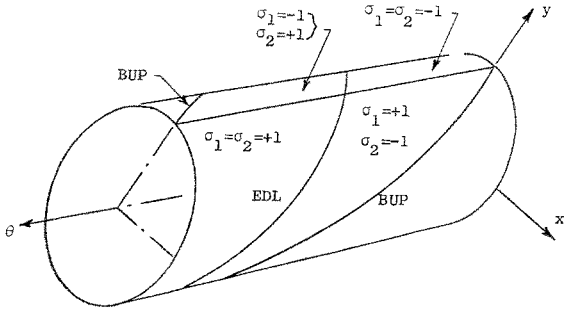

Fig. 2. Terminal strategies on capture circle.

that, because the speeds of the players are equal, the BUP does not intersect the xy-plane at $\phi_0 = \pi/2$, as is the case when P is faster (Ref. 1, Fig. 9.2.2).

The *main equation* or Hamiltonian for the game of kind is written as

$$\min_{\sigma_1} \max_{\sigma_2} [\nu_x \dot{x} + \nu_y \dot{y} + \nu_\theta \dot{\theta}] = 0, \tag{7}$$

where the adjoint vector in this case can be initially normalized to unit magnitude as in Refs. 1 and 2. Substituting (2) into (7) and performing the indicated operations yields

$$\sigma_1 = \text{sign } S \triangleq \text{sign}(\nu_x y - \nu_y x + \nu_\theta), \qquad \sigma_2 = \text{sign } \nu_\theta . \tag{8}$$

The adjoints in turn satisfy the equations $\nabla \dot{\boldsymbol{\nu}} = -\partial H/\partial \mathbf{x}$ or

$$\dot{\nu}_x = -\sigma_1 \nu_y , \qquad \dot{\nu}_y = \sigma_1 \nu_x , \qquad \dot{\nu}_\theta = -\nu_x \cos\theta + \nu_y \sin\theta, \tag{9}$$

where the values at termination of the game of kind are written vectorially as

$$\nabla \boldsymbol{\nu}_0 = [\sin\phi_0 , \cos\phi_0 , 0]. \tag{10}$$

The terminal states in the game of degree are as given by (3), where Ineq. (4) holds. Strategies are given in terms of the adjoints V_x, V_y, V_θ, which are the gradients given in (1). The adjoints satisfy the equations

$$\dot{V}_x = -\sigma_1 V_y , \qquad \dot{V}_y = \sigma_1 V_x , \qquad \dot{V}_\theta = -V_x \cos\theta + V_y \sin\theta, \tag{11}$$

and the terminal values are easily found in terms of the radial relative velocity; i.e., at termination, the main equation can be expressed in terms of polar coordinates, so that

$$V_{r_0} = -1/\dot{r}_0 , \tag{12}$$

where $\dot{r}_0$ is given by (4). Hence, denoting the retrograde derivative by a superscript circle, we have

$$V_{x_0} = \sin(\phi_0)/\mathring{r}_0 , \qquad V_{y_0} = \cos(\phi_0)/\mathring{r}_0 , \qquad V_{\theta_0} = 0, \tag{13}$$

where $\mathring{r}_0$ is positive when $\phi_0 < 2\theta_0$.

1.3. Terminal Strategies. When the barrier ends with $\theta_0 = 0$, two cases must be distinguished. For $\phi_0 \neq 0$, the terminal state vector is

$$\mathbf{x}_0 = [\beta \sin\phi_0 , \beta \cos\phi_0 , 0], \tag{14}$$

which, with (8) and (10), shows that both switch functions are zero at this time. The retrograde derivatives, however, give

$$dS/d(-t) = \mathring{S}_0 = v_{x_0} = \sin\phi_0\,, \qquad dv_\theta/d(-t) = \mathring{v}_{\theta_0} = \sin\phi_0\,, \tag{15}$$

so that, just before tangency, $\sigma_1 = \sigma_2 = \text{sign}\, x_0$. That is, P and E are turning in the same direction.

The second possibility when $\theta_0 = 0$ is that $\phi_0 = 0$, and here (15) shows that the first derivatives are also zero. The second retrograde derivatives, however, show that the strategies just before termination are $\sigma_1 = \text{sign}\,\sigma_1$ and $\sigma_2 = \text{sign}\,\sigma_2$. Consequently, three possible strategies for each player ($\sigma_i = -1, 0, +1$) satisfy the necessary conditions, and further tests of these nine possible strategy pairs will be made using the retrograde solutions of the next section.

For barrier termination when $\theta_0 = 2\phi_0 \neq 0$, the terminal state is

$$\mathbf{x}_0 = [\beta \sin\phi_0\,, \beta\cos\phi_0\,, 2\phi_0], \tag{16}$$

while the terminal adjoint is as given in (10). Again, both switch functions are zero at termination, and the retrograde derivatives yield

$$\mathring{S} = \sin\phi_0\,, \qquad \mathring{v}_{\theta_0} = \sin(\phi_0 - \theta_0) = -\sin\phi_0\,. \tag{17}$$

These results imply that, if E is not directly in front of or behind P, $\sigma_1 = \text{sign}\,\mathring{S}_0 = \text{sign}\, x_0$; that is, P is turning toward E just before tangency, as might be expected. Furthermore, $\sigma_2 = -\sigma_1$, so that E is turning in the opposite direction, or toward the outward normal to the capture circle. This is also physically appealing; and it may be noted that, in the homicidal chauffeur game, E's velocity is parallel to the terminal radius vector; analogies between these two games are often useful.

For the game of degree, the switch functions are identical in form to (8); i.e., the strategies are determined by

$$\sigma_1 = \text{sign}(V_x y - V_y x + V_\theta), \qquad \sigma_2 = \text{sign}\, V_\theta\,, \tag{18}$$

and (3) and (13) show that both switch functions are zero at termination. The retrograde derivatives, however, are

$$\mathring{S}_0 = V_{x_0} = \sin(\phi_0)/\mathring{r}_0\,, \qquad \mathring{V}_{\theta_0} = -\sin(\theta_0 - \phi_0)/\mathring{r}_0\,. \tag{19}$$

For $x_0 > 0$, these imply that P's strategy is $\sigma_1 = +1$ (P is turning right), while E's switch function is $\sigma_2 = -\text{sign}\sin(\theta_0 - \phi_0)$. That is, $\sigma_2 = -1$ if $2\phi_0 < \theta_0 < \phi_0 + \pi$, and $\sigma_2 = +1$ if $\phi_0 + \pi < \theta_0 < 2\pi$. The line $\theta_0 = \phi_0 + \pi$ on the capture circle (see Fig. 2) thus represents a

dispersal line for E (or EDL), and either extreme strategy is optimal here.

On the other hand, if $x_0 = \phi_0 = 0$, the second retrograde derivative gives P's strategy as

$$\sigma_1 = \operatorname{sign} \overset{\circ\circ}{S}_0 = \operatorname{sign} \sigma_1 , \tag{20}$$

which implies that $\sigma_1 = 0$ or ± 1. For this same condition, E's strategy is unique, $\sigma_2 = -\operatorname{sign} \sin \theta_0$, while the multiple strategies for P are a consequence of the *universal surface* which intersects the front of the capture circle along the line $x = 0$, $y = \beta$. P's strategy changes for termination on either side of this line, as shown in Fig. 2.

1.4. General Solutions. We have shown that optimal controls are at extreme values, unless a switch function is identically zero. For reference purposes, the solutions corresponding to these controls are given here. When $\sigma_2 = -\sigma_1 = \pm 1$, so that E is turning in a direction opposite to P's, the retrograde solutions to (2) are found in terms of the terminal state as

$$\begin{aligned} x &= x_0 \cos \tau + \sigma_1[1 - \cos \tau + y_0 \sin \tau + \cos \theta - \cos(\theta_0 + \sigma_1 \tau)], \\ y &= y_0 \cos \tau + \sin \tau - \sigma_1[x_0 \sin \tau + \sin \theta - \sin(\theta_0 + \sigma_1 \tau)], \\ \theta &= \theta_0 + 2\sigma_1 \tau. \end{aligned} \tag{21}$$

Similarly, when $\sigma_2 = \sigma_1 = \pm 1$, the retrograde solutions are

$$\begin{aligned} x &= x_0 \cos \tau + \sigma_1[1 - \cos \tau + y_0 \sin \tau + \cos(\theta_0 + \sigma_1 \tau) - \cos \theta_0], \\ y &= y_0 \cos \tau + \sin \tau - \sigma_1[x_0 \sin \tau + \sin(\theta_0 + \sigma_1 \tau) - \sin \theta_0], \\ \theta &= \theta_0 . \end{aligned} \tag{22}$$

We will find that singular arcs for P are sometimes optimal, such that $\sigma_1 = 0$ and $\sigma_2 = \pm 1$. For this case, the paths are given by

$$\begin{aligned} x &= x_0 - \sigma_2(\cos \theta - \cos \theta_0), \\ y &= y_0 + \tau + \sigma_2(\sin \theta - \sin \theta_0), \\ \theta &= \theta_0 - \sigma_2 \tau. \end{aligned} \tag{23}$$

While it is not hard to write solutions to the adjoint equations (11), it is found that discontinuities in the adjoints occur in the retrograde paths before the switch functions change sign. This is due to the dispersal surface for E (Ref. 1, Chapter 6), which intersects the capture circle at the

EDL shown in Fig. 2. The implication is that strategies (and resulting solutions) can be found without explicit knowledge of the adjoint vector components.

2. Game of Kind

We have shown that the barrier encloses the capture circle, and we have mentioned that an evader's dispersal line intercepts the retrograde solution for the barrier. Consequently, as mentioned in Section 1.3, the general retrograde solutions can be used, with the various terminal conditions (14) and (16), to determine possible trajectory surfaces and the associated switching lines for the two players.

2.1. Termination with $\theta_0 = 0$. We have determined in (15) that, unless $\phi_0 = 0$, $\sigma_1 = \sigma_2 = \text{sign } x_0$. Using the general solutions (22) for $x_0 = \beta \sin \phi_0 > 0$ yields the retrograde motion as

$$x = \beta \sin(\phi_0 + \tau), \qquad y = \beta \cos(\phi_0 + \tau), \tag{24}$$

which shows that the radial separation remains constant in this *safe-contact* motion (Fig. 3a). The real-space interpretation is more easily understood (Fig. 3b). It is readily shown that, when E is initially behind P, it is E who chooses the direction of travel on the capture circle. That is, the point $\mathbf{x} = [0, -\beta, 0]$ is an evader's dispersal point, since, if $|\sigma_2| \neq 1$ and $\sigma_1 = \pm 1$, the equations of motion will show that $\dot{r} < 0$. Therefore, E must choose $\sigma_2 = \pm 1$ to avoid penetrating the capture circle, and P's strategy must be $\sigma_1 = \sigma_2$ in order to keep $\dot{r} = 0$; that is, if $\sigma_1 \neq \sigma_2$, then $\dot{r} > 0$, and P would then lose contact with E.

In the special terminal case $\theta = \phi_0 = 0$, as mentioned in Section 1.3, nine possible sets of strategies satisfy the necessary conditions. The retrograde solutions of Section 1.4 can be used to show that $r(\tau) \geqslant \beta$ for six of these strategy pairs (namely, $\sigma_2 = \pm 1$ and $\sigma_1 = 0$ or ± 1). The case $\sigma_1 = \sigma_2 = 0$ obviously leaves $r(\tau) = \beta$, and the remaining

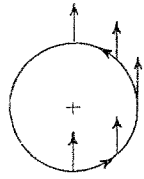

Fig. 3a. Safe contact with $\sigma_1 = \sigma_2 = +1$ (relative space).

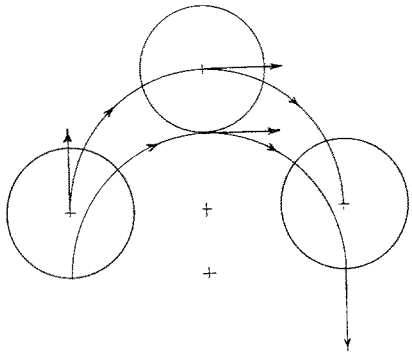

Fig. 3b. Safe contact with $\sigma_1 = \sigma_2 = +1$ (real space).

two cases are related to the strategies $\sigma_2 = 0$ and $\sigma_1 = \pm 1$. The solutions corresponding to these strategies show that $\dot{r}_0 = \overset{\circ\circ}{r}_0 = 0$ and that the third retrograde derivative is *negative*, which implies that these strategies cannot be optimal for the terminal condition being examined.

When the barrier terminates at $\theta_0 = \phi_0 = 0$, with $\sigma_1 = 0$ and $\sigma_2 = \pm 1$, the paths in relative and real space will resemble those shown in Figs. 4a and 4b for $\sigma_2 = +1$. Here, P is following a *singular arc*, and E's trajectory in relative space is termed a universal line (or UL). As mentioned in Section 1.1, the retrograde barrier paths terminate at an evader's dispersal point. This means that, at a certain point on the retrograde path shown in Figs. 4a and 4b, E can instead choose to turn *left*, causing P to turn *right* and resulting in safe contact, as will be discussed in the next section.

The final possibility for termination of the barrier at $\mathbf{x} = [0, \beta, 0]$ is given by the strategies $\sigma_1 = -\sigma_2 = \pm 1$. Here, P and E are turning in opposite directions before termination, and again the retrograde

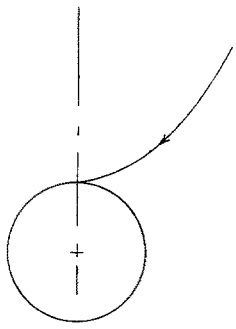

Fig. 4a. Safe contact with $\sigma_1 = 0$, $\sigma_2 = +1$ (relative space).

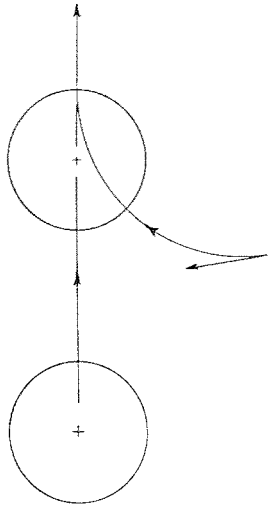

Fig. 4b. Safe contact with $\sigma_1 = 0$, $\sigma_2 = +1$ (real space).

solutions given by (21) are curtailed at an evader's dispersal line. The determination of this EDL will be discussed in Section 2.3.

2.2. Termination with $\theta_0 = 2\phi_0$. When the barrier intersects the capture circle at a nonzero angle ϕ_0, we have seen in (5) that the angular state must be $\theta_0 = 2\phi_0$. The strategies at termination were found in (17) to be $\sigma_1 = -\sigma_2 = \text{sign } x_0$; so, if $x_0 > 0$, the retrograde solutions are given by (21) as

$$\begin{aligned} x &= 1 - \cos\tau + \beta \sin(\phi_0 + \tau) - \cos(\theta_0 + \tau) + \cos\theta, \\ y &= \sin\tau + \beta \cos(\phi_0 + \tau) + \sin(\theta_0 + \tau) - \sin\theta, \\ \theta &= \theta_0 + 2\tau. \end{aligned} \tag{25}$$

As in the other barrier trajectories discussed, a dispersal point marks the end of this trajectory, as is suggested by Fig. 5. This is an illustration in real space of the dispersal point phenomenon, drawn for $\beta = 0.5$. In this typical case, E contacts the capture circle at the angular coordinate ϕ_0 by choosing $\sigma_2 = -1$, or at the coordinate $\phi_0 = 0$ by choosing $\sigma_2 = +1$. P's strategies will be $\sigma_1 = +1$ for the first choice, while the second choice entails a two-part strategy for P ($\sigma_1 = -1, 0$), the terminal portion of which includes the UL discussed in Section 2.1.

This example illustrates that barrier termination points at the EDP require simultaneous consideration of the various combinations of

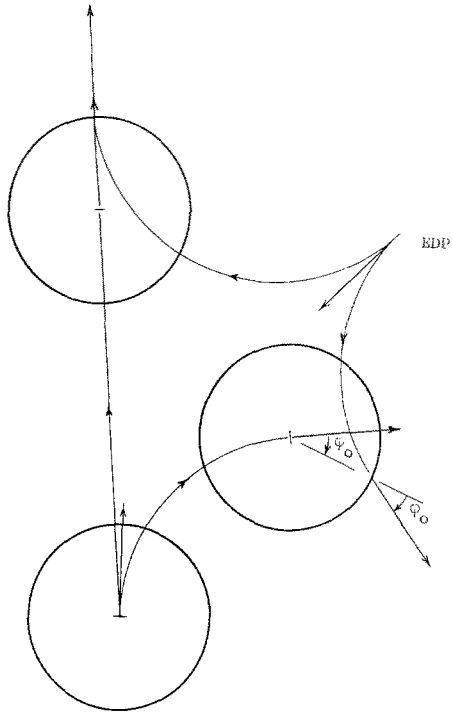

Fig. 5. Evader's dispersal point, $\theta = -3\pi/4$.

safe-contact strategies determined in Section 1.3. That is, the retrograde paths given by (25) are optimal only until an EDP is reached, and the adjoints and both switch functions are discontinuous at this point. Notice that the time-to-go from the EDP is different for the two paths in Fig. 5, but that this characteristic applies only to dispersal points on the *barrier*.

2.3. Barrier. By combining the notions of the two previous sections, the barrier (or envelope of capturable states) can be constructed. We first consider the determination of a point on the barrier for which $x = 0$ and $\theta = \pi$. Here, the players are initially moving toward each other, and obviously E must choose either extreme strategy, $\sigma_2 = \pm 1$. P's initial strategy is $\sigma_1 = -\sigma_2$, and this strategy holds until the time-to-go is $\tau = \tau_1$, when P's velocity is tangent to E's minimum-turn circle. Subsequent relative motion is along the UL, and P maintains $\sigma_1 = 0$ until tangential contact at $x_0 = \phi_0 = 0$ (Fig. 6a). The symmetry here implies that the optimal times-to-go are equal for either choice of σ_2.

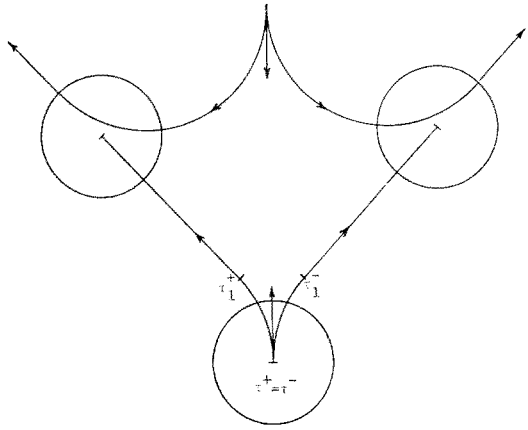

Fig. 6a. Barrier strategies, $\theta = \pi$, $x = 0$.

That is, at this point on the EDL, $\tau^+ = \tau^-$, where the superscripts correspond to E's choice of turn rate, $\sigma_2 = \pm 1$. Also shown in the figure are the points at which $\sigma_1 = 0$; these are labelled $\tau_1{}^+$ and $\tau_1{}^-$. The superscript notation is used to distinguish two optimal strategies and paths which begin at a dispersal point. A process of elimination shows that, for this initial condition, barrier termination must occur at $\phi_0 = 0$, to be in accord with the various possibilities discussed in Section 2.1.

For a *nearby* point on the barrier, where E's initial velocity is oriented by the same angle $\theta = \pi$, the terminal state $\mathbf{x}_0 = [0, \beta, 0]$ will be the same, as shown in Fig. 6b. This *nearby* point is shown for $x > 0$, and E's strategy here is unique, since the EDL at $\theta = \pi$ is located at $x = 0$.

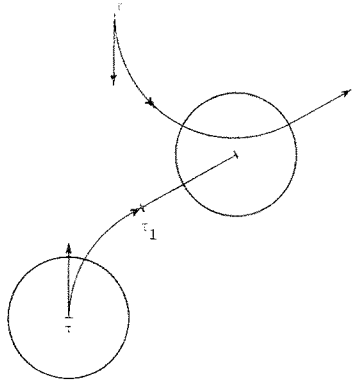

Fig. 6b. Barrier strategies, $\theta = \pi$, $x > 0$.

The small changes in τ_1 and τ due to this small change in x can be noted by comparing Fig. 6b to the right-hand paths of Fig. 6a.

As P's switch time τ_1 is reduced, the locus of barrier initial conditions at $\theta = \pi$ will change; and, when this time-to-go is $\tau_1 = 0$, P does not use $\sigma_1 = 0$. E's initial condition for this circumstance is $\mathbf{x} = [\beta, 2, \pi]$, as can be seen by sketching the real-space paths of P and E for the strategies $\sigma_1 = +1$ and $\sigma_2 = -1$. The subsequent barrier locus at $\theta = \pi$ is given by a vertical line in relative space, which is tangent to the right edge of the capture circle. For initial conditions on this vertical line, E contacts the capture circle with the terminal state given by (16) of Section 1.3, that is, $\phi_0 = \theta_0/2 > 0$.

Thus, a section of the barrier at $\theta = \pi$ has the Gothic arch shape shown in Fig. 7. For $\theta = \pi$ and for other values of θ not too far from π, P's path will include a UL ($\sigma_1 = 0$) for either of E's strategies from the EDL. The calculation for such two-part strategies begins by fixing the initial value of θ and solving two simultaneous equations for τ^+ and τ^-.

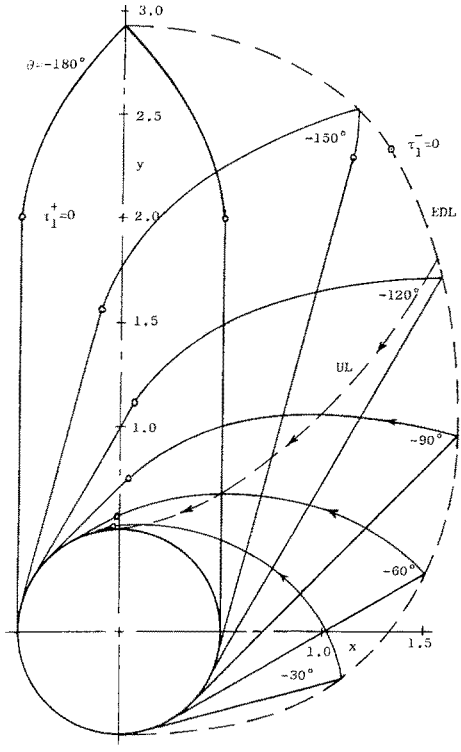

Fig. 7. Cross sections of the barrier, $\beta = 0.5$.

Thus, using (21) and (23) successively for the left-hand path, we have

$$\theta^+(\tau_1^+, \tau^+) = \tau_1^+ - 2\tau^+ = \theta, \tag{26}$$

where τ_1^+ is the time-to-go when P switches from $\sigma_1 = -1$ to $\sigma_1 = 0$. The right-hand path, for which E chooses $\sigma_2 = -1$ at the EDL, also ends at $\mathbf{x} = [0, \beta, 0]$, but different switch and termination times are implied; i.e., (22) and (23) give

$$\theta^-(\tau_1^-, \tau^-) = -\tau_1^- + 2\tau^- = \theta. \tag{27}$$

These two equations are solved for τ_1^+ and τ_1^-, and the coordinates of the dispersal point are given by equating $x^+ = x^-$ and $y^+ = y^-$. Thus, using (21)–(23), we have

$$\begin{aligned} x^+(\tau_1^+, \tau^+) &= -1 - (\beta + \tau_1^+)\sin(\tau^+ - \tau_1^+) + 2\cos(\tau^+ - \tau_1^+) - \cos(2\tau^+ - \tau_1^+), \\ x^-(\tau_1^-, \tau^-) &= 1 + (\beta + \tau_1^-)\sin(\tau^- - \tau_1^-) - 2\cos(\tau^- - \tau_1^-) + \cos(2\tau^- - \tau_1^-). \end{aligned} \tag{28}$$

Substituting from (26) and (27) for τ_1^+ and τ_1^- then gives

$$\begin{aligned} x^+(\tau^+, \theta) &= -1 - \cos\theta + (\beta + \theta + 2\tau^+)\sin(\theta + \tau^+) + 2\cos(\theta + \tau^+), \\ x^-(\tau^-, \theta) &= 1 + \cos\theta + (\beta - \theta + 2\tau^-)\sin(\theta - \tau^-) - 2\cos(\theta - \tau^-). \end{aligned} \tag{29}$$

Similar equations are found for $y^+(\tau^+)$ and $y^-(\tau^-)$; and, when the coordinates are equated, a numerical solution is possible for τ^+ and τ^-, and the dispersal point $x(\theta)$ and $y(\theta)$.

When $\tau_1^- \leqslant 0$, the implication is that, for this value of θ, E does not arrive at the UL, and $\sigma_1 \neq 0$. In place of (27), we then have, using (25),

$$\theta^-(\phi_0, \tau^-) = 2\phi_0 + 2\tau^- = \theta. \tag{30}$$

For $\beta = 0.5$, this change in the terminal condition turns out to be required when θ is in the interval $-123° < \theta \leqslant 0°$, approximately, and here both P and E have constant strategies from the EDL to termination.

The result of the barrier-computation procedure which has been described is shown in Fig. 7, and the following details are noteworthy: (i) the sections of the capture region are shown for $-\pi \leqslant \theta \leqslant 0$, and symmetry can give the contours for $0 \leqslant \theta \leqslant \pi$; (ii) when E is on the UL, shown as a dashed line intersecting several of the θ-contours, P's control is $\sigma_1 = 0$, while E takes $\sigma_2 = +1$ until termination at $\phi_0 = \theta_0 = 0$, as in Fig. 4; (iii) when E is initially on the curved

portion of a $\theta = \text{const}$ section, the resulting two-stage trajectories include the UL, and terminate at $\phi_0 = \theta_0 = 0$; (iv) when E is initially on the straight portion of a section, P's control is $\sigma_1 = \pm 1$ until termination at $\phi_0 = \theta_0/2 \neq 0$.

This figure also implies the barrier strategies of both P and E. That is, if E is on the barrier to the left (counter-clockwise) of the EDL, then $\sigma_2 = +1$; and, if E is to the right of the EDL, $\sigma_2 = -1$. P's strategy is $\sigma_1 = +1$ when E is below the UL, and $\sigma_1 = -1$ if E is above this line. The UL trajectories can be preceded by paths for which $\sigma_1 = \pm 1$. However, since $\sigma_2 = +1$, tributary paths are shown in Fig. 7 only for $\sigma_1 = +1$, such that θ is constant. The tributary paths which join the UL from above are not shown, since for these paths θ is changing with time.

3. Game of Degree

When $\mathbf{x}$ is inside the barrier, capture of E is possible, and the minmax strategies of P and E are required as functions of $\mathbf{x}$. Retrograde solutions will be used to locate a dispersal surface for E and a universal surface for P, such that the capture region is subdivided into various subregions. The result is that the players' controls are known as functions of $\mathbf{x} = [x, y, \theta]$.

3.1. Evader's Dispersal Surface. As in the game of kind, it is intuitively clear that, when E is initially on the y axis and headed toward P, E must choose $\sigma_2 = \pm 1$. That is, the y axis coincides with the evader's dispersal surface (or EDS) when $\theta = \pi$. P's minimizing strategy is to turn in E's direction ($\sigma_1 = -\sigma_2$), then switching to $\sigma_1 = 0$ such that capture occurs with E at the most forward position of the capture circle, but with $\theta_0 \neq 0$. These strategies are optimal, according to the implications of (19) and (20). That is, if P did *not* switch to $\sigma_1 = 0$, capture would occur with $\sigma_1 = -\text{sign } x_0$, which contradicts the terminal condition of (19).

For other nearby values of θ, the EDS is located by using the equations which are implied by the equal times-to-go (τ) through use of two different strategies. That is, $\tau^+ = \tau^- = \tau$, and

$$x^+(\tau_1^+, \theta_0^+, \tau) = x^-(\tau_1^-, \theta_0^-, \tau), \qquad y^+(\tau_1^+, \theta_0^+, \tau) = y^-(\tau_1^-, \theta_0^-, \tau), \quad (31)$$

where τ_1^+ and τ_1^- are the times-to-go when P's strategy becomes $\sigma_1 = 0$.

Using the solutions to the two angular equations corresponding to these two strategy pairs, we have

$$\theta^+ = \theta_0{}^+ - 2\tau + \tau_1{}^+, \qquad \theta^- = \theta_0{}^- + 2\tau - \tau_1{}^-. \tag{32}$$

Thus, $\theta_0{}^+$ and $\theta_0{}^-$ can be eliminated from (31), so that, with $\theta^+ = \theta^- = \theta$,

$$\begin{aligned} x^- - x^+ &= 2[1 + (1 - \cos\tau)\cos\theta] + (\beta + \tau_1{}^-)\sin(\tau - \tau_1{}^-) \\ &\quad + (\beta + \tau_1{}^+)\sin(\tau - \tau_1{}^+) - \cos(\tau - \tau_1{}^-) - \cos(\tau - \tau_1{}^+) = 0, \\ y^- - y^+ &= -2(1 - \cos\tau)\sin\theta + (\beta + \tau_1{}^-)\cos(\tau - \tau_1{}^-) \\ &\quad - (\beta + \tau_1{}^+)\cos(\tau - \tau_1{}^+) + \sin(\tau - \tau_1{}^-) - \sin(\tau - \tau_1{}^+) = 0. \end{aligned}$$

Numerical solution of these equations for $\tau_1{}^+$ and $\tau_1{}^-$ as functions of (θ, τ) then produces a dispersal point locus (x, y), as long as both switch times turn out to fall in the interval $0 \leqslant \tau_1{}^+, \tau_1{}^- \leqslant \tau$. Otherwise, P may initially turn right regardless of E's strategy from the EDS, then

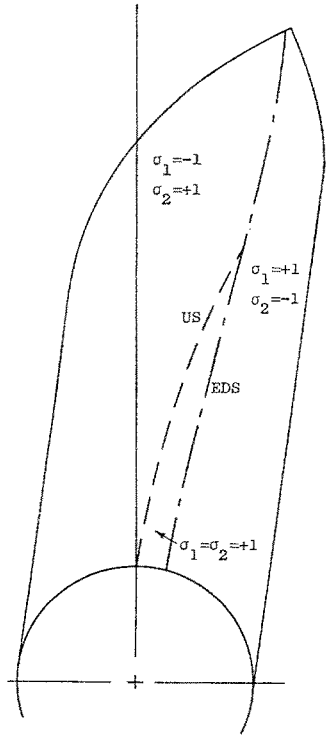

Fig. 8a. Optimal strategies in the capture region, $\beta = 0.5$, $\theta = -165°$.

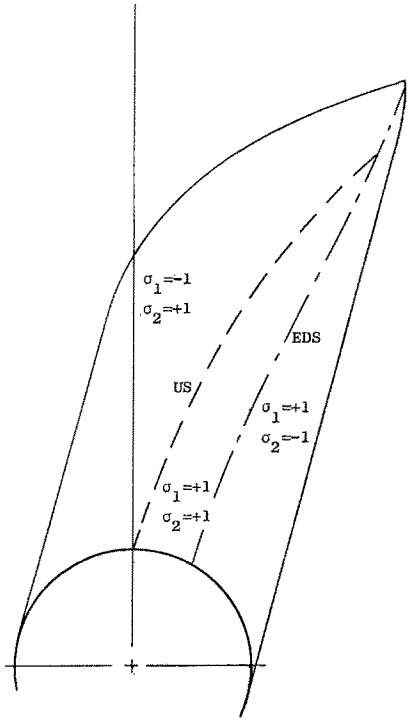

Fig. 8b. Optimal strategies in the capture region, $\beta = 0.5$, $\theta = -150°$.

switching to $\sigma_1 = 0$ or not, depending on whether or not $\tau_1 > 0$. The numerical calculations in these various cases are essentially the same, however. That is, they all use the equalities $x^+ = x^-$, $y^+ = y^-$, and $\theta^+ = \theta^- = \theta$ as required on the EDS, and it is only necessary to use the proper sets of solutions with $\tau^+ = \tau^-$ to eliminate the intermediate unknowns, which are $\theta_0{}^+$, $\theta_0{}^-$ and either $\tau_1{}^\pm$ or $\phi_0{}^\pm$.

3.2. Pursuer's Universal Surface. A universal surface (or US) for P exists at those points for which P's optimal strategy is $\sigma_1 = 0$. On this surface, the equations of relative motion have the solutions given in (23). But we have shown that the terminal conditions when $\sigma_1 = 0$ must be $x_0 = 0$, $y_0 = \beta$, with θ_0 arbitrary. Restricting attention to $\sigma_2 = 1$ (since for $-\pi < \theta_0 \leqslant 0$, this US originates to the left of the EDS, as in Fig. 2), we see that the retrograde solutions are

$$x = \cos\theta_0 - \cos(\theta_0 - \tau), \quad y = \beta + \tau - \sin\theta_0 + \sin(\theta_0 - \tau), \quad \theta = \theta_0 - \tau, \tag{33}$$

and these paths are optimal from termination at θ_0 back to the EDS or the barrier.

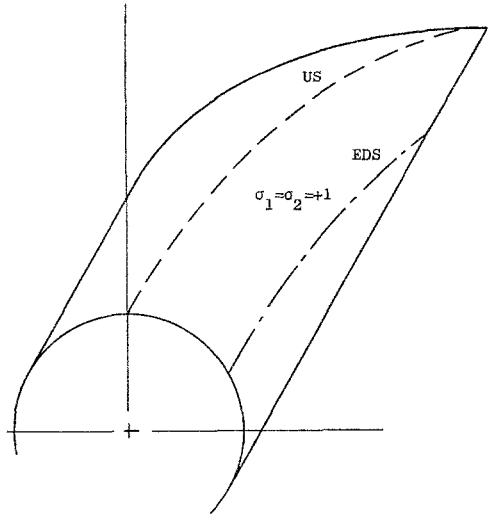

Fig. 8c. Optimal strategies in the capture region, $\beta = 0.5$, $\theta = -120°$.

In order to display the intersection of the US with planes of constant θ, as was done for the EDS, θ_0 is eliminated from Eqs. (33-1) and (33-2). The resulting line $x(\theta, \tau)$, $y(\theta, \tau)$ can then be drawn through each section of the capture region between the capture circle and the EDS or the barrier. When E is above the US, P turns hard left, and conversely if E is below the US. When E arrives at the US, $\sigma_1 = 0$, and the resulting path (a singular arc in the game of degree) remains on the US until capture at $x_0 = 0$.

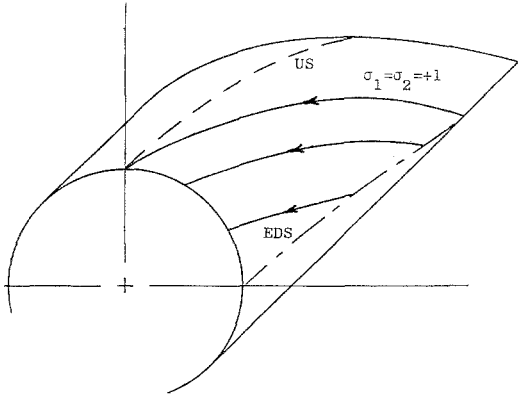

Fig. 8d. Optimal strategies in the capture region, $\beta = 0.5$, $\theta = -90°$.

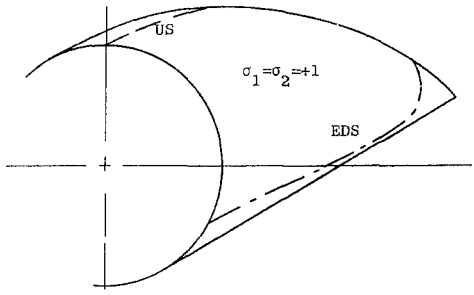

Fig. 8e. Optimal strategies in the capture region, $\beta = 0.5$, $\theta = -60°$.

3.3. Strategies of the Game of Degree. Results of the previous calculations are presented as $\theta =$ const sections of the state space. As shown in Figs. 8a–8f for $\beta = 0.5$, the EDS and US are smooth surfaces which vary continuously with θ. Across the EDS, σ_2 switches, and across the US, σ_1 switches.

Certain interesting features of the surface may be noted. Thus, for θ_0 near π, the US extends from the point $[0, \beta, \theta_0]$ only to the EDS, as shown in Figs. 8a and 8b. At $\theta = \pi$, the US has length zero, and the EDS coincides with the y axis, as noted earlier. The EDS extends from the EDL shown on the capture cylinder in Fig. 2 to the vicinity of the upper corner of the capture volume. This corner is the EDL in the game of kind. For θ_0 between 0° and −140°, approximately, the US and EDS no longer intersect, as shown in Fig. 8c. Trajectories, of course, can be shown in these sectional figures only when $\sigma_1 = \sigma_2 = 1$, such that $\dot{\theta} = 0$; representative paths for these strategies are shown in Fig. 8d. The sharp curve in the EDS for θ near −60° is an unexpected result which can be verified by plotting real-space trajectories of the players, when E's initial condition is on this line.

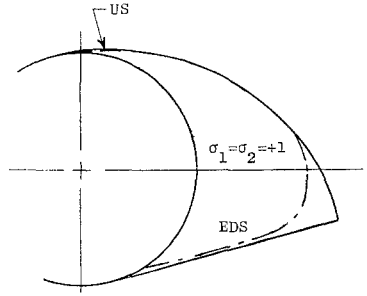

Fig. 8f. Optimal strategies in the capture region, $\beta = 0.5$, $\theta = -30°$.

4. Conclusions

The game of two identical cars represents a first step in the generalization of the second-order homicidal chauffeur game. The present study shows that optimal strategies for P and E can be determined as functions of the three-dimensional state, and that the higher order of the problem does not require the introduction of any new types of *exceptional* surfaces. Thus, when the capture region is finite, the only exceptional surfaces appear to be a universal surface for P and a dispersal surface for E. This is exactly the result found for the homicidal chauffeur game, when the capture region is finite and the speed ratio is between $\sqrt{(1-\beta^2)}$ and 1 (Ref. 2).

Many of the exceptional lines which occurred in the homicidal chauffeur game were in fact possible only because of the pedestrian's unlimited maneuverability. It is conjectured that the general solution to the *smoother* game of two cars will involve fewer exceptional surfaces, even when P and E have different speeds and turn radii.

References

1. Isaacs, R., *Differential Games*, John Wiley and Sons, New York, 1965.
2. Merz, A., *The Homicidal Chauffeur—A Differential Game*, Stanford University, Department of Aeronautics and Astronautics, Ph.D. Thesis, 1971.